Bashir et al. *Advances in Difference Equations* (2019) 2019:334
https://doi.org/10.1186/s13662-019-2272-4

Advances in Difference Equations
a SpringerOpen Journal

RESEARCH Open Access

# Comparison of fractional order techniques for measles dynamics

Amna Bashir[1], Muhammad Mushtaq[1], Zain Ul Abadin Zafar[2*], Kashif Rehan[3] and Rana Muhammad Akram Muntazir[1]

*Correspondence:
zainzafar@ucp.edu.pk;
zainzafar2016@hotmail.com
[2]Faculty of Information Technology, University of Central Punjab, Lahore, Pakistan
Full list of author information is available at the end of the article

**Abstract**

A mathematical model which is non-linear in nature with non-integer order $\phi$, $0 < \phi \leq 1$ is presented for exploring the SIRV model with the rate of vaccination $\mu_1$ and rate of treatment $\mu_2$ to describe a measles model. Both the disease free $\mathcal{F}_0$ and the endemic $\mathcal{F}^*$ points have been calculated. The stability has also been argued for using the theorem of stability of non-integer order differential equations. $\mathcal{R}_0$, the basic reproduction number exhibits an imperative role in the stability of the model. The disease free equilibrium point $\mathcal{F}_0$ is an attractor when $\mathcal{R}_0 < 1$. For $\mathcal{R}_0 > 1$, $\mathcal{F}_0$ is unstable, the endemic equilibrium $\mathcal{F}^*$ subsists and it is an attractor. Numerical simulations of considerable model are also supported to study the behavior of the system.

**Keywords:** Measles model; Stability; Generalized Euler Method; Grunwald Letnikov Method; Binomial Coefficients; Fractional Derivatives; Adams–Bashforth–Moulton Method; Piece wise Continuous Argument (PWCA)

## 1 Introduction

Measles is a worldwide disease. Both epidemic and endemic occurrences are known. The highest incidence is in winter and spring. It is a respiratory disease (measles) triggered by a virus known as paramyxovirus. It is generally held that measles is not a good reason to consult a doctor. Instead, the parents prefer to visit a temple. The poorer community has the higher occurrence of infection at lower age [1]. All this adds up to the problems of the child with measles. No specific treatment is available. General measures consist of isolation, cough sedatives, vasoconstrictor nasal drops, antipyretics, attention to eye and mucous membrane of mouth, antihistaminic for itching, and maintenance of proper fluid and dietary intake. In the case bacterial infection is superimposed, proper antibiotics should be given. Antiviral agents are not of proven value. Gamma globulins, hyper immune gamma globulins and steroids are of doubtful value [2]. The symptoms of the measles appear 10 to 14 days after a person is infected with the measles virus. Worldwide, measles vaccination has been effective, reducing measles deaths by 78% from an estimated 562,400 deaths in 2000 to 122,000 in 2012. A few nonlinear models are given in [3–16, 36, 37].

Measles cases have continued to climb into 2019. Preliminary global data shows that reported cases rose by 300% in the first 3 months of 2019, compared to the same period in 2018. In 2017, it caused nearly 110,000 deaths [17]. During 2000–2017, measles vaccination prevented an estimated 21.1 million deaths. Global measles death has decreased by 80% from an estimated 545,000 in 2000 to 110,000 in 2017 [18]. The WHO estimated that 875,000 children died of measles in 1999 [19]. This is 56% of all estimated deaths from vaccine-preventable diseases of childhood for that year, making measles the leading cause of vaccine-preventable child mortality.

In recent years' fractional order derivatives have been introduced in compartment models, replacing ordinary derivatives with fractional derivatives. This has been motivated by the utility of fractional derivatives in incorporating history effects. The geometrical and physical significance of the fractional integral having a complex and real conjugate power-law exponent has been suggested. One somatic implication of the non-integer order in non-integer derivatives concerns the index of memory [7]. Moreover, non-integer calculus displays a vivacious part of superdiffusive and subdiffusive measures, which make it an obliging instrument in the learning of syndrome transmission [6]. As integer order differential equations cannot authoritatively depict the exploratory and field estimation information, as an alternative approach fractional order differential equations mock-ups are at the moment being widely applied [20]. The fractional modeling is a beneficial approach which has been practiced to understand the comportment of syndromes; the non-integer derivative is a generalization of the ordinary derivative. The non-integer order is global in nature whereas the ordinary derivative is local. The fractional order may offer extra 'freedom' to amend the model to factual data from particular patients; specifically, that the fractional order index subsidizes positively to better fits of the patients' information. The benefit of FDE systems over ODE frameworks is that they allow for more notable degrees of flexibility and they include a memory effect in the model. In other words, they give a superb manoeuvre for the portrayal of memory and traditional gears which were not considered in the established non-fractional order prototypical. Fractional calculus has heretofore been applied in epidemiological research [6]. Also, fractional order models retain memory so a fractional order differential equation gives us a more realistic way to model measles. A significant role of modeling enterprises is that it can alert us to the paucities in our up-to-date understanding of the epidemiology of numerous infectious ailments, and propose critical queries for analysis and data that need to be collected. Lately, it has been applied to analyze dengue internal transmission model, bovine babesiosis disease and a tick population model, a HIV/AIDS epidemic model and the Lengyel–Epstein chemical reaction model [6, 7, 20, 21]. Although the operating of the non-integer approach is more complex than the out-dated one, there are numerical approaches for cracking systems of DEs which are nonlinear. Recently, a majority of the dynamical frameworks centered on the non-fractional order calculus have been altered into the non-integer order domain with regard of the additional degrees of opportunity and the malleability which can be utilized to resolutely fit the test information this being much superior over anything concerned with integer order molding.

As of not long ago, FC was considered as a fairly exclusive numerical hypothesis without applications, yet over the most recent couple of decades there has been a blast of research efforts on the use of FC to assorted scientific fields extending from the material science of dispersion and shift in weather conditions phenomena, to control frameworks to economics and financial matters. Without a doubt, at present, applications and/or efforts identified with FC have showed up in at least the following fields [22]:

- Non-integer control of engineering systems.
- Development of calculus of variations and optimal control to non-integer dynamic structures.
- Numerical and analytical tools and procedures.
- Essential investigations of the electrical, mechanical, and thermal constitutive relations and other properties of numerous engineering materials, for instance foams, gels, animal tissues, and viscoelastic polymers, and their engineering and scientific applications.
- Essential understanding of diffusion and wave phenomena, their measurements and verifications, comprising applications to plasma physics (such as diffusion in Tokamak).
- Biomedical and bioengineering applications.
- Thermal modeling of engineering structures for instance brakes and machine tools.
- Signal and image processing.

This article contains five sections. The overview is the first section wherein we present some antiquities of non-integer calculus. In Sect. 2, we will present details of the concept of FDEs. In Sect. 3, we deliberate on the non-integer order model allied with the dynamics of measles model. Qualitative dynamics of the considerable system is resolute using elementary reproduction number. We provide the local stability analysis of the disease free equilibrium (DFE) and endemic equilibrium (EE) points. In Sect. 4, numerical replications are shown to confirm the core outcomes and the conclusion is in Sect. 5.

## 2 Beginnings

For numerous ages, there have been many demarcations that address the idea of non-integer derivatives [6, 7]. In this section, the Caputo (C), Riemann Liouville (RL) and Grunwald–Letnikov (GL) fractional derivative (FD) demarcations are presented. Firstly, we present the definition of the RL non-integer integral,

$$J^{\varsigma} g(z) = \bigl(\Gamma(\varsigma)\bigr)^{-1} \int_0^z \frac{g(s)}{(z-s)^{1-\gamma}}\, ds, \tag{1}$$

where $\gamma > 0$, $g \in L^1(R^+)$, and $\Gamma(\cdot)$ is the Gamma function.

The RL derivative is

$$\begin{aligned} D_R^{\gamma} g(z) &= \frac{d^m}{dz^m}\bigl[J^{m-\gamma} g(z)\bigr] \\ &= \frac{1}{\Gamma(m-\gamma)} \frac{d^m}{dz^m} \int_0^z \frac{g(s)}{(z-s)^{1-m+\gamma}}\, ds, \quad m-1 \le \gamma < m. \end{aligned} \tag{2}$$

The Caputo fractional derivative is given by

$$D_C^{\gamma} g(x) = J^{M-\varsigma}\left[\frac{d^M}{dx^M} g(x)\right] = \frac{1}{\Gamma(M-\varsigma)} \int_0^x (x-s)^{M-\varsigma-1} g^{(M)}(s)\, ds, \tag{3}$$

where $M > \gamma$, $\forall M \in Z^+$.

The GL derivative is given by

$$ {}_{a}D^{\gamma}_{x_k} g(x) = \lim_{h\to 0} \frac{1}{h^{\gamma}} \sum_{j=0}^{[\frac{x-a}{h}]} (-1)^{j} \binom{\gamma}{j} g(x-jh), \tag{4} $$

where [ · ] means the non-fractional quantity.

The Laplace transform of the Caputo FD is written

$$ \mathcal{L}\left[D^{\varphi}_{C} g(x)\right] = s^{\varphi} G(s) - \sum_{j=0}^{n-1} g^{(j)}(0) s^{\varphi-j-1}. \tag{5} $$

The Mittag-Leffler (ML) function is defined by using an infinite power series:

$$ E_{\alpha,\beta}(s) = \sum_{k=0}^{\infty} \frac{s^{k}}{(\alpha k+\beta)}. \tag{6} $$

The Laplace transform of the functions is

$$ \mathcal{L}\left[t^{\beta-1} E_{\alpha,\beta}\left(\pm a t^{\alpha}\right)\right] = \frac{s^{\alpha-\beta}}{s^{\alpha} \mp a}. \tag{7} $$

Let $\alpha, \beta > 0$ and $z \in \mathbb{C}$, and the Mittag-Leffler functions mollify the equality given by Theorem 4.2 in [6],

$$ E_{\alpha,\beta}(z) = z E_{\alpha,\alpha+\beta}(z) + \frac{1}{\Gamma(\beta)}. \tag{8} $$

**Definition 1** "A function $F$ is Hölder continuous if there are non-negative amounts $W$, $\nu$ such that

$$ \left\|F(p) - F(\tau)\right\| \le W \|p-\tau\|^{\nu}, \tag{9} $$

for all $p$, $\tau$ in the purview of $F$ and $\nu$ is the Hölder exponent. We represent the space of Hölder-continuous functions by $W^{0,\nu}$" [7].

Consider the fractional order system:

$$ D^{\varphi}_{C} \varpi(h) = z(h, \varpi). \tag{10} $$

We have the initial condition $\varpi(0) = \varpi_0$ where $D^{\varsigma}_{C}\varpi(h) = (D^{\varsigma}_{C}\varpi_1(h), D^{\varsigma}_{C}\varpi_2(h), D^{\varsigma}_{C}\varpi_3(h), \ldots, D^{\varsigma}_{C}\varpi_m(h))^{T}$, $0 < \varsigma < 1$, $\varpi(h) \in \mathcal{F} \subset R^{m}$, $h \in [0, T)$ $(T \le \infty)$, $\mathcal{F}$ is an open set, $0 \in \mathcal{F}$, and $z : [0, T) \times \mathcal{F} \to R^{m}$ is not discontinuous in $h$ and placates the Lipschitz condition:

$$ \left\|z\left(h, \varpi'\right) - z\left(h, \varpi''\right)\right\| \le P \left\|\varpi' - \varpi''\right\|, \quad \mathfrak{H} \in [0, T) \tag{11} $$

for all $\varpi', \varpi'' \in \Omega \subset \mathcal{F}$, where $P > 0$ is a Lipschitz constant.

**Theorem 1** *"Let the solution of* (10) *be* $u(h)$, $h \in [0, H)$. *If there exists a vector function* $\varpi = (\varpi_1, \varpi_2, \ldots, \varpi_m)^H : [0, H) \to \mathcal{F}$ *such that* $\varpi_i \in G^{0,\nu}$, $\varsigma < \varpi < 1$, $i = 1, 2, \ldots, m$ *and*

$$D_C^{\varphi} \varpi \leq g(h, \varpi), \quad \mathfrak{H} \in [0, H]. \tag{12}$$

*If* $\varpi(0) \leq\leq u_0$, $u_0 \in \mathcal{F}$, *then* $w \leq\leq u$, $h \in [0, H]$*"* [7].

Let $g : \mathcal{F} \to R^m$, $\mathcal{F} \in R^m$, we study the following system of non-integer order:

$$D_C^{\varsigma} x(\tau) = g(x), \quad x(0) = x_0. \tag{13}$$

**Definition 2** We say that $\mathcal{F}$ is an equilibrium point of (13), iff, $g(\mathcal{F}) = 0$.

*Remark* 1 When $\varsigma \in (0, 1)$, the fractional system $D_C^{\varsigma} x(\tau) = g(x)$ has the identical equilibrium points as the arrangement $\frac{dx(\tau)}{dt} = g(x)$ [7].

**Definition 3** "The equilibrium point $\mathcal{F}$ of autonomous (13) is said to be stable if, for all $\epsilon > 0$, $\varepsilon > 0$ exists such that if $\|x_0 - \mathcal{F}\| < \varepsilon$, then $\|x - \mathcal{F}\| < \epsilon$, $t \geq 0$; the equilibrium point $\mathcal{F}$ of autonomous (13) is said to be asymptotically unwavering if $\lim_{t\to\infty} x(\tau) = \mathcal{F}$" [7].

**Theorem 2** *"The equilibrium points of system* (13) *are locally asymptotically stable if all eigenvalues* $\lambda_i$ *of Jacobian matrix* $J$, *calculated in the equilibrium points, satisfy* $|\arg(\lambda_i)| > \varsigma \frac{\pi}{2}$*"* [6, 16].

## 3 Mathematical model

Many researchers have discussed a measles model, like the SEIR measles model discussed in [23], the SIR measles model discussed in [24, 25], and the SVIER measles model discussed in [26]. Some authors have discussed the model using ordinary differential equations and some using fractional order differential equations to control the measles model. In this paper, we are going to study a non-integer order SIRV epidemic model with vaccination and treatment rates. We assume that the total populace $N(t)$ is divided into four compartments, $S(t)$, $I(t)$, $R(t)$ and $V(t)$. Here, $S(t)$ be the proportion of populace which are susceptible at time $t$, $I(t)$ be the populace proportion which are infected at time at time $t$, $R(t)$ be the populace proportion which are recovered and $V(t)$ be the populace proportion which are vaccinated at time $t$. Let $b$ denote the birth rate; $\beta$ denotes the disease transmission rate, which is supposed to occur with straight contact among infectious and susceptible hosts. We denote the natural death degree $d(N)$ for the populace. For convenience, $d$ is supposed to be continuous, which does not disagree with natural death rates. We assume $\alpha$ to be the disease-induced death rate and there exist $\mu_1$ and $\mu_2$ which in turn signify the proportion of susceptibles that are vaccinated per unit time and the proportion of infectives that are picked per unit time. $(1 - \mu_1)$ denotes the unvaccinated rate. The dynamical system signifying the epidemic blowout in the populace is set by the subsequent

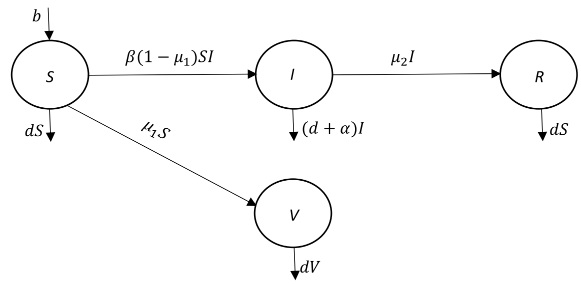


**Figure 1** Flow chart of the model

system of non-linear ODEs [27] and the flow cart is given in Fig. 1. We have

$$\begin{cases} \frac{dS}{dt} = b - \beta(1-\mu_1)SI - (d+\mu_1)S, \\ \frac{dI}{dt} = \beta(1-\mu_1)SI - (d+\mu_2+\alpha)I, \\ \frac{dR}{dt} = \mu_2 I - dR, \\ \frac{dV}{dt} = \mu_1 S - dV, \end{cases} \tag{14}$$

with $S(0) = S_0 > 0$, $I(0) = I_0 > 0$, $R(0) = R_0 > 0$ and $V(0) = V_0 > 0$.

Note that individuals in $V$ are different from those in both $S$ and $R$. The immune system will create antibodies against the disease because vaccination is taken care of during this process. The vaccination individuals, before obtaining immunity, still have the possibility of infection while contacting with infected individuals. Individuals in $V$ may be assumed to move into $R$ when they gain immunity. We assume that $b$, $\beta$, $d$, $\alpha$, $\mu_1$ and $\mu_2$ are all non-negative constants. We must note that, for the ailment free case (i.e. $I = 0$), the total populace has logistic growth.

Adding all the equations of (14) we have

$$\begin{aligned} \frac{d(S+I+R+V)}{dt} &= \frac{dS}{dt} + \frac{dI}{dt} + \frac{dR}{dt} + \frac{dV}{dt} \\ &= b - \beta(1-\mu_1)SI - (d+\mu_1)S + \beta(1-\mu_1)SI \\ &\quad - (d+\mu_2+\alpha)I + \mu_2 I - dR + \mu_1 S - dV \\ &= b - d(S+I+R+V) - \alpha I. \end{aligned}$$

Let $S + I + R + V = N$, then

$$\begin{aligned} &\frac{dN}{dt} = b - dN - \alpha I, \\ &\frac{dN}{dt} \le b - dN. \end{aligned}$$

On solving the above equation

$$N(t) \le \frac{b}{d}\left(1 - e^{-dt}\right) + N(0)e^{-dt},$$

where $N(0)$ represents the initial value of the respective variables. Then $0 \leq N(t) \leq \frac{b}{d}$ as $t \to \infty$. Therefore, $\frac{b}{d}$ is an upper bound of $N(t)$ provided $N(0) \leq \frac{b}{d}$. This means that the population size is not constant or in other words the population is dynamic.

The following equations can be transformed by the given model [27]:

$$\begin{cases} \frac{dS}{dt} = b - \beta(1-\mu_1)SI - (d+\mu_1)S, \\ \frac{dI}{dt} = \beta(1-\mu_1)SI - (d+\mu_2+\alpha)I, \\ \frac{dR}{dt} = \mu_2 I - dR, \\ \frac{dV}{dt} = \mu_1 S - dV, \\ \frac{dN}{dt} = b - Nd - \alpha I. \end{cases} \tag{15}$$

In system (15) $R$ is not involved in any other equations except in the third equation so it can be removed from system (15) and we obtain the system (16):

$$\begin{cases} \frac{dS}{dt} = b - \beta(1-\mu_1)SI - (d+\mu_1)S, \\ \frac{dI}{dt} = \beta(1-\mu_1)SI - (d+\mu_2+\alpha)I, \\ \frac{dV}{dt} = \mu_1 S - dV, \\ \frac{dN}{dt} = b - Nd - \alpha I. \end{cases} \tag{16}$$

If we solve the system (16) then we can evaluate the factor $R(t)$, because $R(t) = N(t) - S(t) - I(t) - V(t)$.

### 3.1 Fractional order model

The system of non-integer order non-linear ODEs for the system (16), with $\phi \in (0,1]$, is given by

$$\begin{cases} \frac{d^{\phi_1}S}{dt^{\phi_1}} = b - \beta(1-\mu_1)SI - (d+\mu_1)S, \\ \frac{d^{\phi_2}I}{dt^{\phi_2}} = \beta(1-\mu_1)SI - (d+\mu_2+\alpha)I, \\ \frac{d^{\phi_3}V}{dt^{\phi_3}} = \mu_1 S - dV, \\ \frac{d^{\phi_4}N}{dt^{\phi_4}} = b - Nd - \alpha I, \end{cases} \tag{17}$$

with

$$S(0) = S_0, \qquad I(0) = I_0, \qquad V(0) = V_0 \quad \text{and} \quad N(0) = N_0 \tag{18}$$

as the initial conditions. We use for all the values of fractional order $\phi_1 = \phi_2 = \phi_3 = \phi_4 = \phi$. If all the values are the same then the system is called a commensurate model. If some values of $\phi$ are the same and some are different or all the values are different, then the system is called an incommensurate model.

In this manuscript we use a commensurate model to observe the dynamic behavior of the measles.

### 3.2 Non-negative solution

Symbolize $R^4_+ = \{X \in R^4 : X \geq 0\}$ and $X(t) = (S, I, V, N)^T$. For the evidence of the non-negative solution, study the subsequent theorem and corollary.

**Theorem 3** (Generalized mean value theorem) *"Let $f(x) \in C(0,a)$ and $D^{\alpha} f(x) \in C(0,a]$, for $0 < \alpha \leq 1$. Then we have*

$$f(x) = f(0+) + \frac{1}{\Gamma(\alpha)} \bigl(D^{\alpha} f\bigr)(\xi)(x)^{\alpha} \tag{19}$$

*with $0 \leq \xi \leq x$, $\forall x \in (0,\alpha]$"* [8, 28].

*Proof* The proof is given in [28]. □

**Corollary 1** *"Suppose that $f(x) \in C[0,a]$ and $D^{\alpha} f(x) \in C(0,\alpha]$ for $0 < \alpha \leq 1$. It is clear from Theorem 3 that if $D^{\alpha} f(x) \geq 0$, $\forall x \in (0,a)$, then $f(x)$ is non-decreasing, and if $D^{\alpha} f(x) \leq 0$, $\forall x \in (0,a)$, then $f(x)$ is non-increasing for all $x \in [0,a]$"* [8].

**Theorem 4** *"There is a unique solution $X(t) = (S,I,V,N)^{T}$ for the initial value problem given (17) at $t \geq 0$ and the solution remains in $R_{+}^{4}$"* [8].

*Proof* It is easy to understand the existence and uniqueness of the result of the initial value problem (17)–(18) in $(0,\infty)$. We will display that the purview $R_{+}^{4}$ remains positively invariant.

Then

$$\begin{aligned}
\left.\frac{d^{\phi_1} S}{dt^{\phi_1}}\right|_{S=0} &= b \geq 0, \\
\left.\frac{d^{\phi_2} I}{dt^{\phi_2}}\right|_{I=0} &= 0, \\
\left.\frac{d^{\phi_3} V}{dt^{\phi_3}}\right|_{V=0} &= \mu_1 S \geq 0, \\
\left.\frac{d^{\phi_4} N}{dt^{\phi_4}}\right|_{N=0} &= b - \alpha I \geq 0,
\end{aligned}$$

on each hyperplane bounding the non-negative orthant and, because of Corollary 1, the result will linger in $R_{+}^{4}$. □

**Lemma** *"Let $u(t)$ be continuous function on $[t_0,\infty]$ satisfying*

$$\frac{d^{\alpha} u(t)}{dt^{\alpha}} \leq -\mu u(t) + \lambda, \qquad u(t_0) = u_{t_0},$$

*where $0 < \alpha < 1$, $(\mu,\lambda) \in R^2$, $\mu \neq 0$ and $t_0 \geq 0$ is the initial time. Then its solution has the form*

$$u(t) = \left(u_0 - \frac{\lambda}{\mu}\right) E_{\alpha}\bigl[-\mu(t-t_0)^{\alpha}\bigr] + \frac{\lambda}{\mu},$$

*where $E_{\alpha}(z)$ is the Mittag-Leffler function with parameter $\alpha$."*

### 3.3 Stability and equilibrium points

Addressing the nonlinear algebraic equations, the equilibrium points of (17) are found:

$$D^{\phi_1}S(t) = D^{\phi_2}I(t) = D^{\phi_3}V(t) = D^{\phi_4}N(t) = 0.$$

System (17) has DFE point $\mathcal{F}_0(\frac{b}{(d+\mu_1)}, 0, \frac{\mu_1}{d}\frac{b}{(d+\mu_1)}, \frac{b}{d})$ if $\mathcal{R}_0 < 1$, while if $\mathcal{R}_0 > 1$, in addition to $\mathcal{F}_0$, there is a positive endemic equilibrium $\mathcal{F}^*(S^*, I^*, V^*, N^*)$ and $S^*$, $I^*$, $V^*$ and $N^*$ are given by

$$\begin{aligned}
S^* &= \frac{\mu_2 + d + \alpha}{\beta(1-\mu_1)} = \frac{b}{\mathcal{R}_0(d+\mu_1)},\\
I^* &= \frac{b\beta(1-\mu_1) - (\mu_1 + d)(\mu_2 + d + \alpha)}{\beta(1-\mu_1)(\mu_2 + d + \alpha)} = \frac{b}{(\mu_2 + d + \alpha)}\left(1 - \frac{1}{\mathcal{R}_0}\right),\\
V^* &= \frac{\mu_1(\mu_2 + d + \alpha)}{d\beta(1-\mu_1)} = \frac{b\mu_1}{\mathcal{R}_0(d+\mu_1)d},\\
N^* &= \frac{b\beta(\mu_2 + d - \mu_1 d - \mu_1\mu_2) + \alpha(\mu_1 + d)(\mu_2 + d + \alpha)}{d\beta(1-\mu_1)(\mu_2 + d + \alpha)} = \frac{(\mu_2 + d + \frac{\alpha}{\mathcal{R}_0})}{(\mu_2 + d + \alpha)},
\end{aligned}$$

where $\mathcal{R}_0$ is the basic reproduction number denoted in [27]

$$\mathcal{R}_0 = \frac{b\beta(1-\mu_1)}{(d + \mu_2 + \alpha)(d + \mu_1)}. \tag{20}$$

The value that $\mathcal{R}_0$ takes can signal the conditions where an epidemic is feasible. $\mathcal{R}_0$, a key threshold number, is used for a stability analysis of (17).

### 3.4 Sensitivity analysis ($\mathcal{R}_0$)

To check the sensitivity of $\mathcal{R}_0$ for each parameter,

$$\begin{aligned}
\frac{\partial\mathcal{R}_0}{\partial b} &= \frac{\beta(1-\mu_1)}{(d+\mu_2+\alpha)(d+\mu_1)} > 0,\\
\frac{\partial\mathcal{R}_0}{\partial \beta} &= \frac{b(1-\mu_1)}{(d+\mu_2+\alpha)(d+\mu_1)} > 0,\\
\frac{\partial\mathcal{R}_0}{\partial d} &= \frac{b\beta(-1+\mu_1)(2d+\mu_2+\mu_1+\alpha)}{(d+\mu_2+\alpha)^2(d+\mu_1)^2} > 0,\\
\frac{\partial\mathcal{R}_0}{\partial \mu_1} &= -\frac{b\beta(1+d)}{(d+\mu_2+\alpha)(d+\mu_1)^2} < 0,\\
\frac{\partial\mathcal{R}_0}{\partial \mu_2} &= -\frac{\beta(1-\mu_1)}{(d+\mu_2+\alpha)^2(d+\mu_1)} < 0,\\
\frac{\partial\mathcal{R}_0}{\partial \alpha} &= -\frac{b\beta(1-\mu_1)}{(d+\mu_2+\alpha)^2(d+\mu_1)} < 0.
\end{aligned}$$

Thus $\mathcal{R}_0$ is increasing with $b$, $\beta$ and $d$, decreasing with $\alpha$, $\mu_2$ and $\mu_1$.

The following theorem describes the stability behavior of system (17) around the DFE point $\mathcal{F}_0$.

### 3.5 Stability behavior around $\mathcal{F}_0$

The following theorem describes the stability behavior of (17) around the infection free equilibrium point $\mathcal{F}_0$.

**Theorem 5** *If* $\mathcal{R}_0 < 1$, *then* (17) *will be locally asymptotically stable around* $\mathcal{F}_0$ *and unstable if* $\mathcal{R}_0 > 1$.

*Proof* For the system (17), the Jacobian matrix around $\mathcal{F}_0$ has the following characteristic equation:

$$(\xi + d + \mu_1)\left(\xi - \beta(1-\mu_1)\frac{b}{(d+\mu_1)} + (d + \mu_2 + \alpha)\right)(\xi + d)(\xi + d) = 0. \tag{21}$$

The eigenvalues of Eq. (21) are

$$\begin{aligned}
&\xi_1 = -(d + \mu_1) < 0, \\
&\xi_2 = \beta(1-\mu_1)\frac{b}{(d+\mu_1)} - (d + \mu_2 + \alpha), \\
&\xi_3 = -d < 0, \\
&\xi_4 = -d < 0.
\end{aligned}$$

Here $\xi_1$, $\xi_3$, and $\xi_4$ are clearly negative. Now we will see that the eigenvalue $\xi_2$ is negative. For disease free equilibrium, $\mathcal{R}_0 < 1$. We have

$$\begin{aligned}
&\beta(1-\mu_1)\frac{b}{(d+\mu_1)} - (d + \mu_2 + \alpha) < 0, \\
&\mathcal{R}_0 = \frac{b\beta(1-\mu_1)}{(d+\mu_2+\alpha)(d+\mu_1)} < 1
\end{aligned}$$

so, $\xi_2 < 0$.

So $\mathcal{F}_0$ is asymptotically stable which is local in nature. □

**Theorem 6** *The endemic equilibrium point is asymptotically stable if* $\mathcal{R}_0 > 1$.

*Proof* The Jacobian matrix for system (17) around $\mathcal{F}_0$ has the following characteristic equation:

$$\left(\xi^2 + \mathcal{R}_0(d+\mu_1)\xi + (\mu_2 + d + \alpha)(\mathcal{R}_0 - 1)(d + \mu_1)\right)(\xi + d)(\xi + d) = 0 \tag{22}$$

The eigenvalues of $J_0(\mathcal{F}^*)$ are

$$\begin{aligned}
&(\xi + d) = 0 \quad \Rightarrow \quad \xi_1 = -d, \\
&(\xi + d) = 0 \quad \Rightarrow \quad \xi_2 = -d
\end{aligned}$$

and

$$\xi^2 + \mathcal{R}_0(d+\mu_1)\xi + (\mu_2+d+\alpha)(\mathcal{R}_0-1)(d+\mu_1) = 0,$$
$$\xi_{3,4} = \frac{-B \pm \sqrt{B^2-4AC}}{2A},$$

where

$$A = 1,$$
$$B = \mathcal{R}_0(d+\mu_1),$$
$$C = (\mu_2+d+\alpha)(\mathcal{R}_0-1)(d+\mu_1).$$

This shows that if $\mathcal{R}_0 > 1$, then $\xi_3 < 0$ and $\xi_4 < 0$, hence the system will be asymptotically stable. □

## 4 Numerical study

In this section we give an illustrative example to authenticate the obtained results on systems (17). We have applied the numerical schemes to examine the paraphernalia of fluctuations in the non-integer order exponent on the qualitative behavior of results. The numerical results congregate to the intended equilibrium states of the fractional SIRV model, when the parameters are constant. Considering four fractional order techniques in the paper, actually we check the best performance wise efficiency of the model. One of the incredible favorable circumstances of the Caputo non-integer derivative is that it permits outmoded initial and boundary conditions to be incorporated in the formation of the issue. Furthermore, its derivative for an invariable is zero. The Caputo non-integer derivative also permits the utilization of the initial and boundary conditions when dealing with real world issues. The Caputo derivative is the most suitable non-integer operator to be utilized in displaying the true issue. We use MATLAB software for the simulations.

Studying the effects of $\phi$ on the dynamics of the non-integer paradigm (17), we address numerous numerical efforts varying the value of the parameters. These simulations reveal the dynamics of the system disturbed using the value of $\phi$. Figures 2, 4, 7, 10, 15–17,

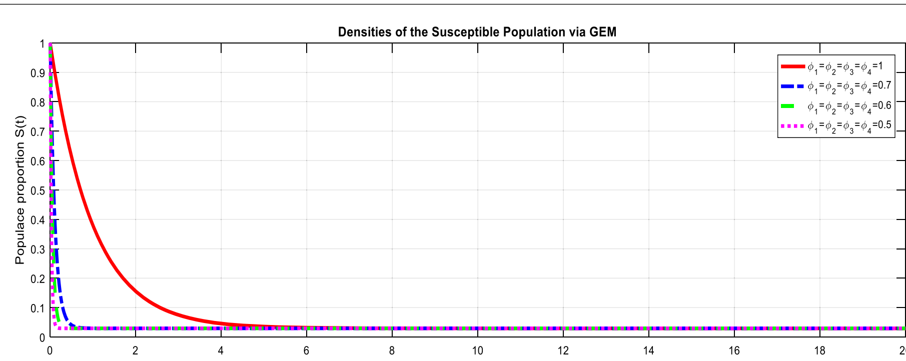


**Figure 2** Dynamic of $S$ by varying the value of $\phi$

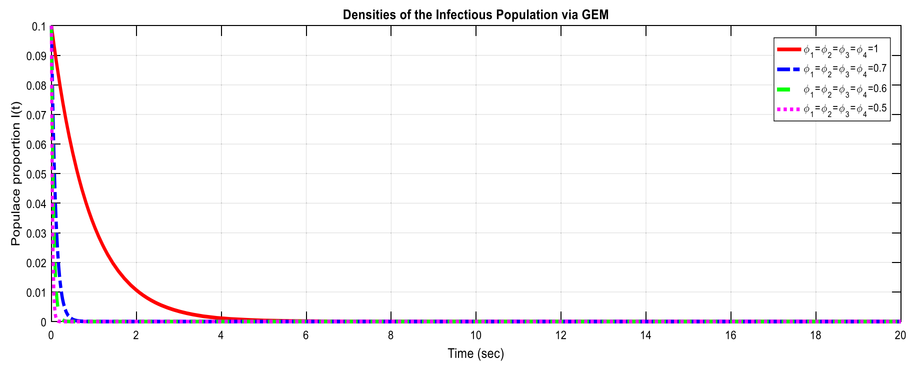


**Figure 3** Dynamic of $I$ by varying the value of $\phi$

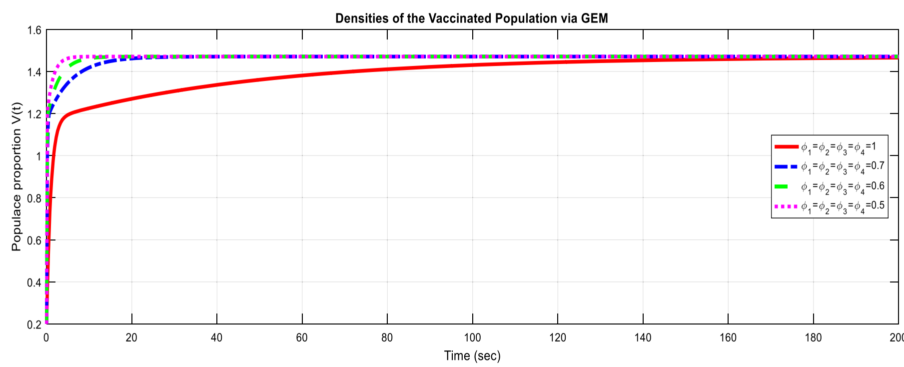


**Figure 4** Dynamic of $V$ by varying the value of $\phi$

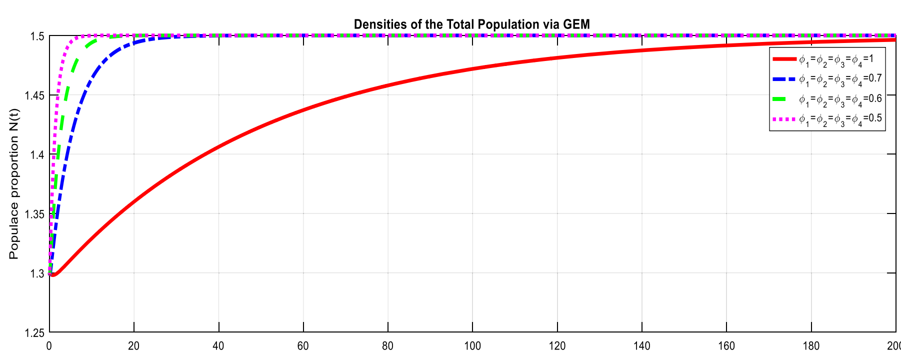


**Figure 5** Dynamic of $N$ by varying the value of $\phi$

20, 21, 26, 28 and 31 depict that, for lower values of $\phi$, the rampant peak is eclectic and less than the true equilibrium points. Figures 3, 5–6, 8–9, 12–14, 18–19, 27, 29–30, 32 and 33 illustrate that, for lower values of $\phi$, the epidemic peak is eclectic and greater for true steady states. Also we find the length of time to approach equilibrium within a given tolerance. The early transient behaviors vary greatly among the methods. Numerical imitations of an amended epidemic model with capricious order show that the non-integer

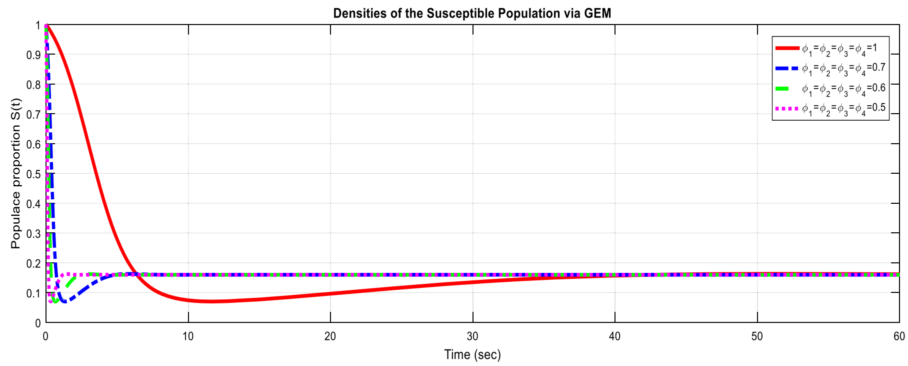


**Figure 6** Dynamic of $S$ by varying the value of $\phi$

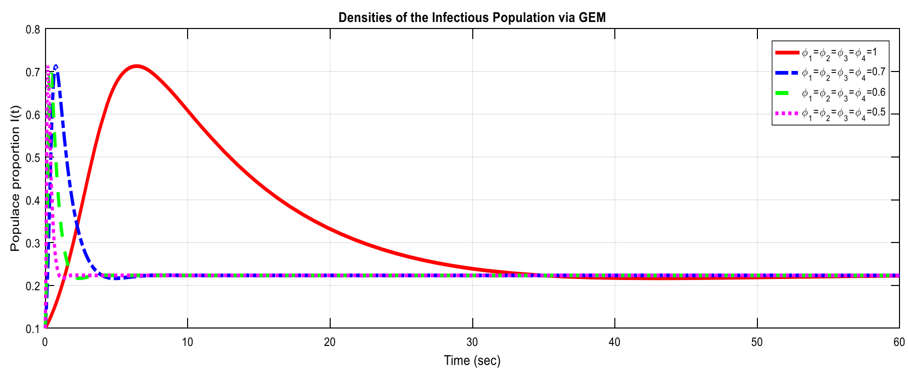


**Figure 7** Dynamic of $I$ by varying the value of $\phi$

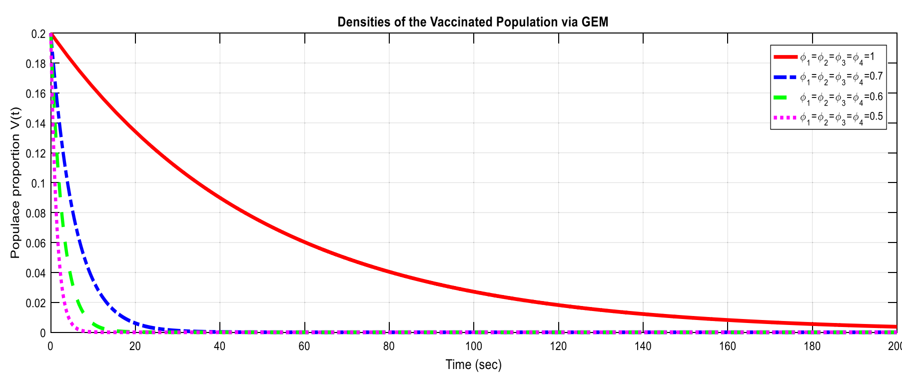


**Figure 8** Dynamic of $V$ by varying the value of $\phi$

order is linked to the relaxation time, i.e., the time engaged to reach equilibrium. The chaotic comportment of the system when the total order of the system is less than four is delineated. A comparison among the four diverse values of non-integer order is shown in Figs. 2–33. For all cases, the ailment evolves to the disease-free and endemic equilibrium points. Figures 2–33 illustrate that the model gradually tends towards the steady state for different $\phi$.

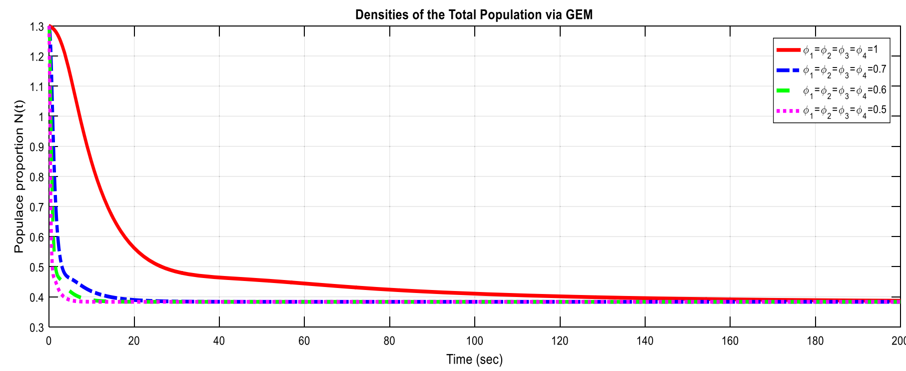


**Figure 9** Dynamic of $N$ by varying the value of $\phi$

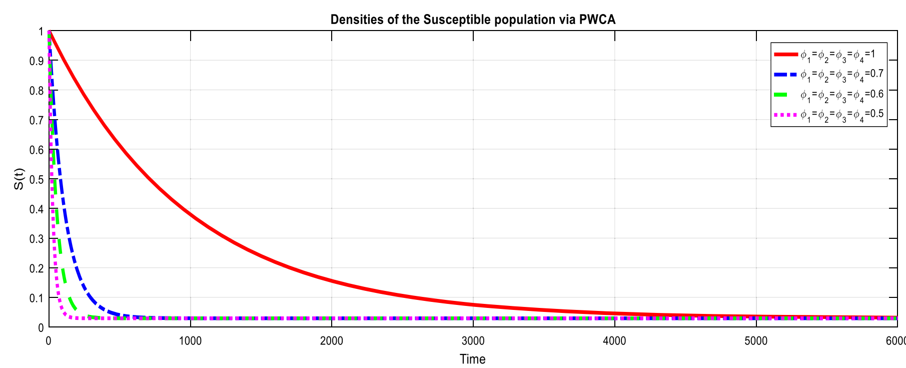


**Figure 10** Dynamic of $S(t)$ by varying the value of $\phi$

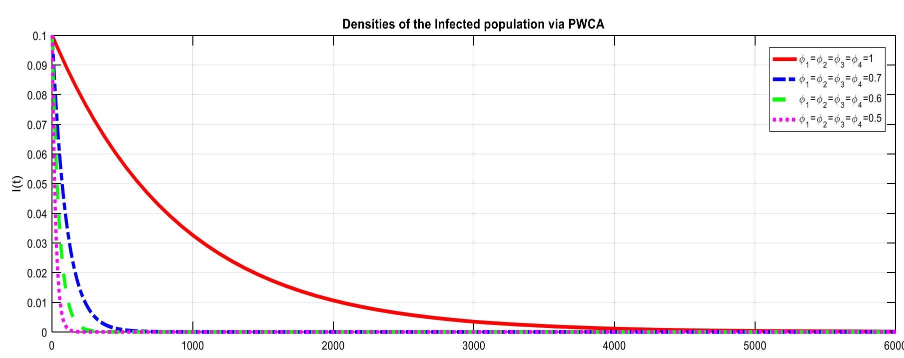


**Figure 11** Dynamic of $I(t)$ by varying the value of $\phi$

### 4.1 Generalized Euler method (GEM)

The generalized Euler method is a generalization of the classical Euler method; for details see [28–32]. The key points of this technique are set as shadows. Let us study the following initial value problem:

$$D_*^{\alpha} y(t) = f\big(y(t), t\big); \qquad y(0) = y_0, \quad 0 < \alpha \leq 1, t > 0 \tag{23}$$

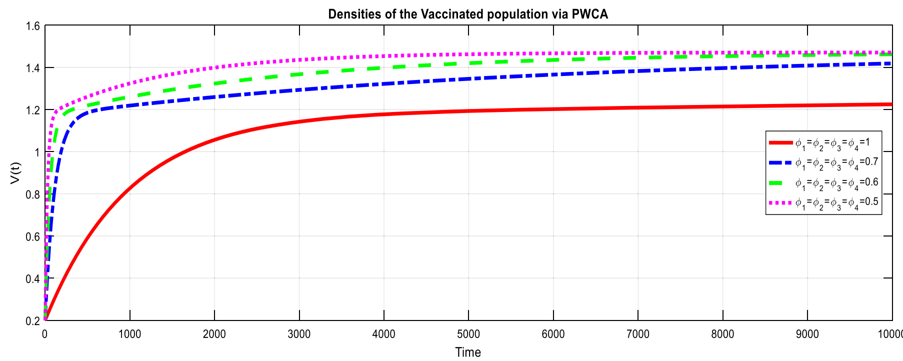


**Figure 12** Dynamic of $V(t)$ by varying the value of $\phi$

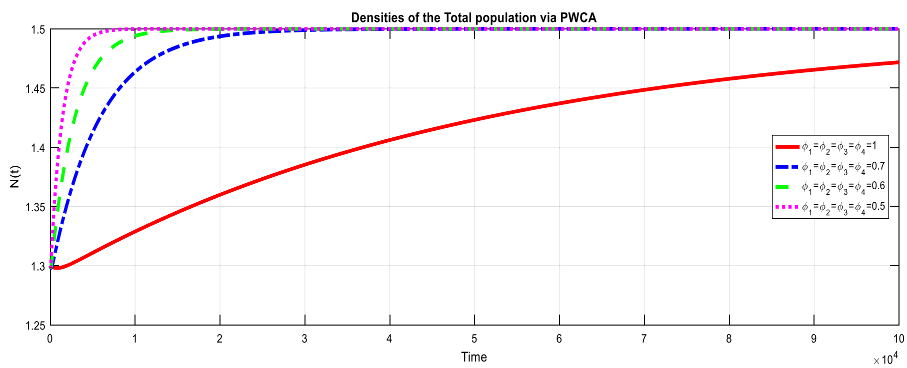


**Figure 13** Dynamic of $N(t)$ by varying the value of $\phi$

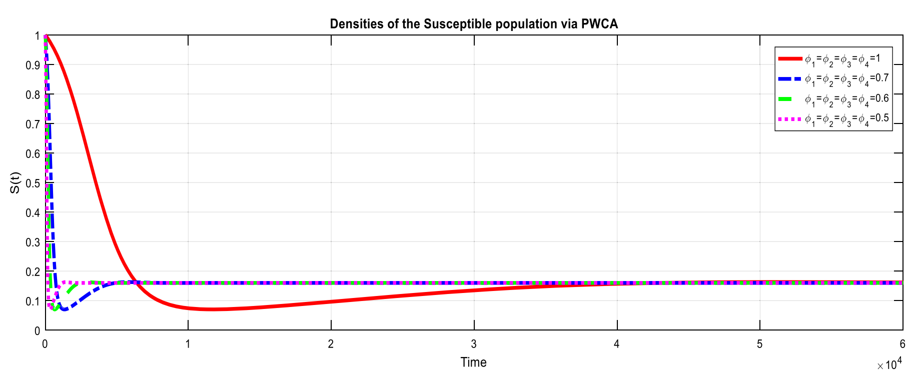


**Figure 14** Dynamic of $S(t)$ by varying the value of $\phi$

where $D_*^\alpha$ is the Caputo FD. Let $[0, a]$ be the interval over which we need to find the result of the problem (23). The interval will be sectioned into $\aleph$ subintervals $[t_j, t_{j+1}]$ of identical width $h = \frac{a}{\aleph}$ by via knots $t_j = jh$, for $j = 0, 1, 2, \dots, \aleph - 1$. The common formulation for GEM when $t_{j+1} = t_j + h$ is

$$y(t_{j+1}) = y(t_j) + \frac{h^\alpha}{\Gamma(\alpha + 1)} f\bigl(y(t_j), t_j\bigr) + O\bigl(h^{2\alpha}\bigr) \tag{24}$$

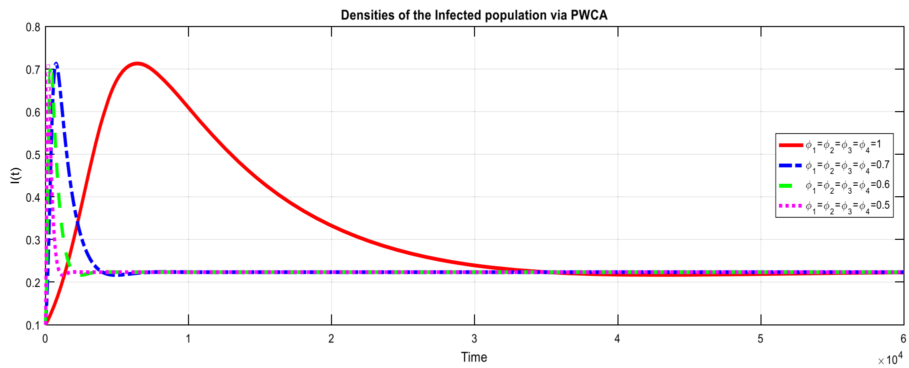


**Figure 15** Dynamic of *I*(*t*) by varying the value of $\phi$

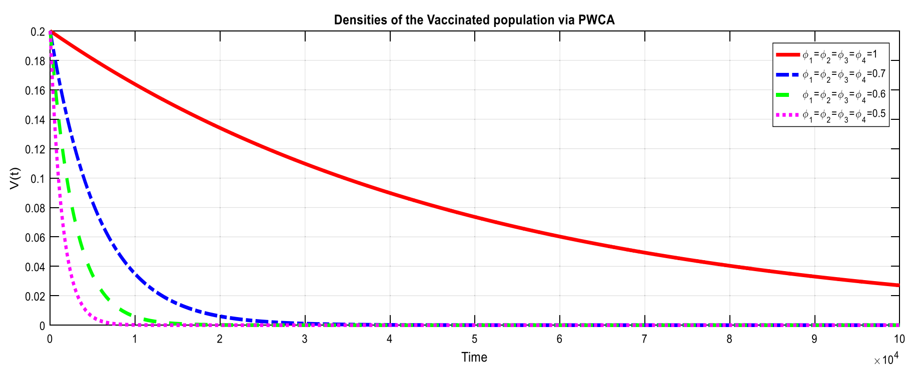


**Figure 16** Dynamic of *V*(*t*) by varying the value of $\phi$

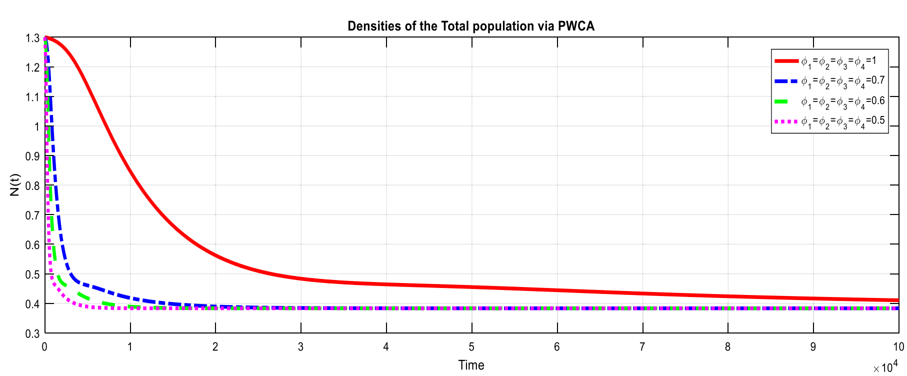


**Figure 17** Dynamic of *N*(*t*) by varying the value of $\phi$

for $j = 0, 1, 2, \dots, \aleph - 1$. If the step size $h$ is selected small enough, then we may neglect the second order term (involving $h^{2\alpha}$) and develop

$$y(t_{j+1}) = y(t_j) + \frac{h^\alpha}{\Gamma(\alpha+1)} f\big(y(t_j), t_j\big). \tag{25}$$

For $\alpha = 1$, Eq. (25) reduces to the classical Euler method.

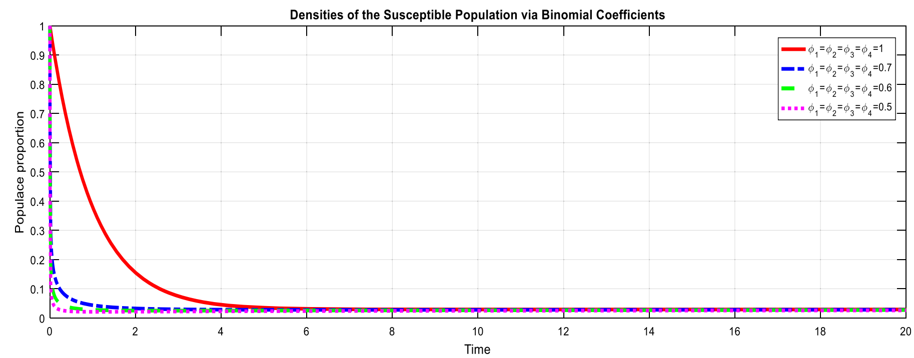


**Figure 18** Dynamic of $S(t)$ by varying the value of $\phi$

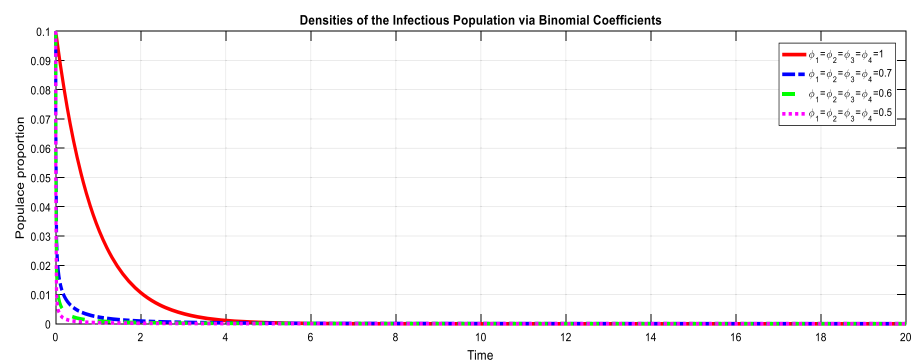


**Figure 19** Dynamic of $I(t)$ by varying the value of $\phi$

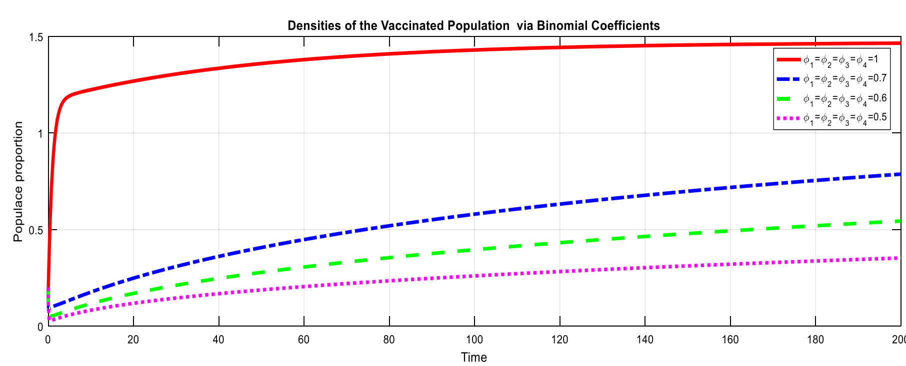


**Figure 20** Dynamic of $V(t)$ by varying the value of $\phi$

So by using the generalized Euler method for system (17), we have the subsequent discretized equations

$$S(t_{\aleph+1}) = S(t_{\aleph}) + \frac{h^{\phi_1}}{\Gamma(\phi_1+1)}\bigl\{b - \beta(1-\mu_1)S(t_{\aleph})I(t_{\aleph}) - (d+\mu_1)S(t_{\aleph})\bigr\},$$

$$I(t_{\aleph+1}) = I(t_{\aleph}) + \frac{h^{\phi_2}}{\Gamma(\phi_2+1)}\bigl\{\beta(1-\mu_1)S(t_{\aleph+1})I(t_{\aleph}) - (d+\mu_2+\alpha)I(t_{\aleph})\bigr\},$$

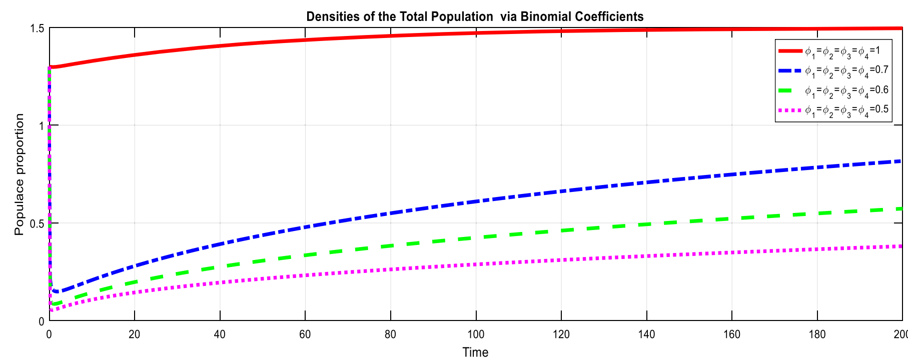


**Figure 21** Dynamic of $N(t)$ by varying the value of $\phi$

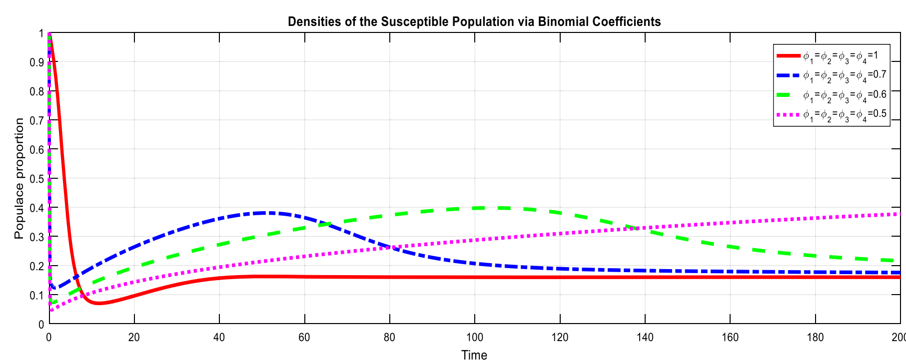


**Figure 22** Dynamic of $S(t)$ by varying the value of $\phi$

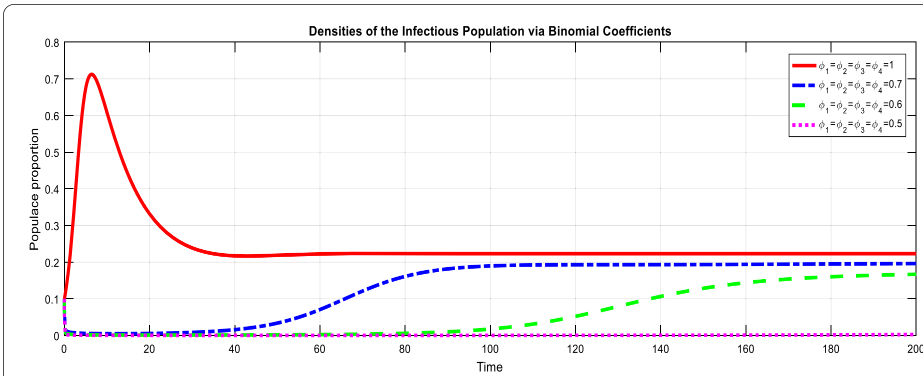


**Figure 23** Dynamic of $I(t)$ by varying the value of $\phi$

$$V(t_{\aleph+1}) = V(t_\aleph) + \frac{h^{\phi_3}}{\Gamma(\phi_3 + 1)}\bigl\{\mu_1 S(t_{\aleph+1}) - dV(t_\aleph)\bigr\},$$

$$N(t_{\aleph+1}) = N(t_\aleph) + \frac{h^{\phi_4}}{\Gamma(\phi_4 + 1)}\bigl\{b - dN(t_\aleph) - \alpha I(t_{\aleph+1})\bigr\}.$$

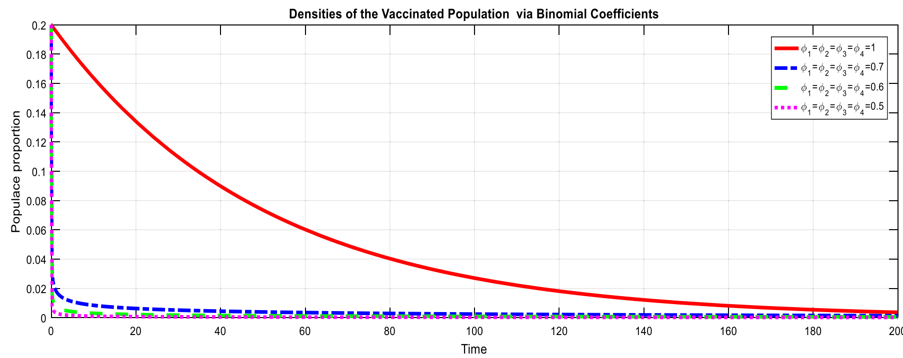


**Figure 24** Dynamic of $V(t)$ by varying the value of $\phi$

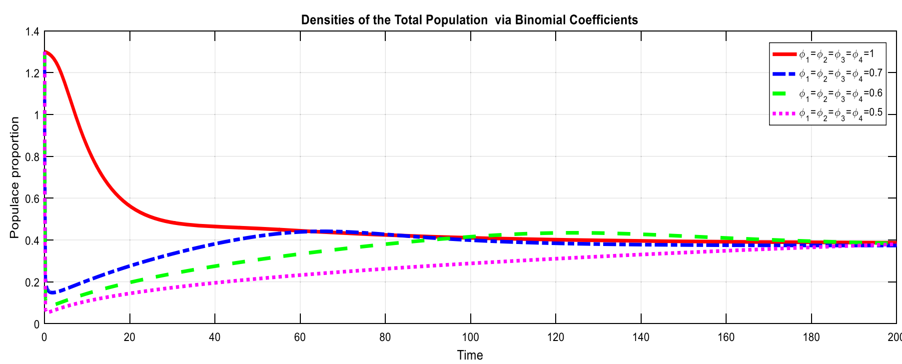


**Figure 25** Dynamic of $N(t)$ by varying the value of $\phi$

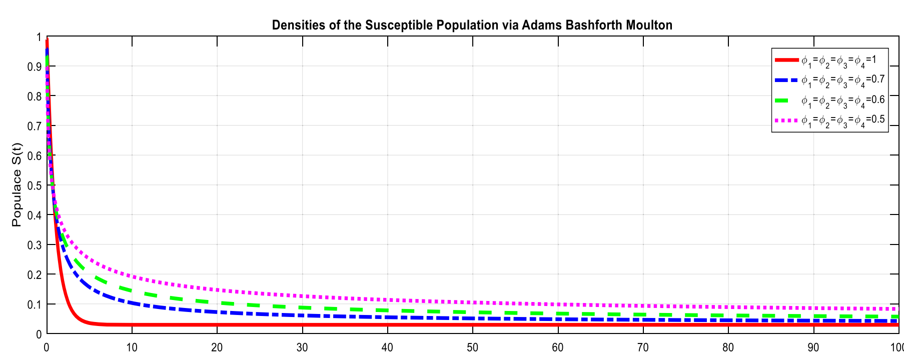


**Figure 26** Dynamic of populace $S(t)$ by varying the value of $\phi$

## 4.2 Piece wise continuous argument method

In this subsection, we apply the discretization process represented in Refs. [33, 34] for a measles model. Here we have used the piece wise constant arguments (PWCA) method to see the behavior of the system (17) by varying the parameters and order of the system.

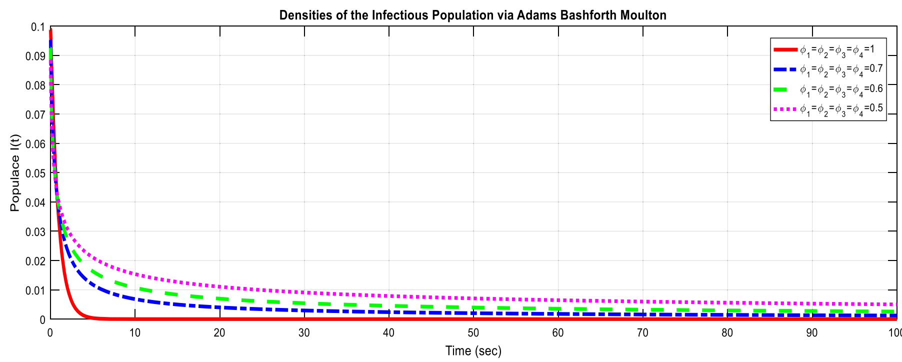


**Figure 27** Dynamic of populace *I*(*t*) by varying the value of $\phi$

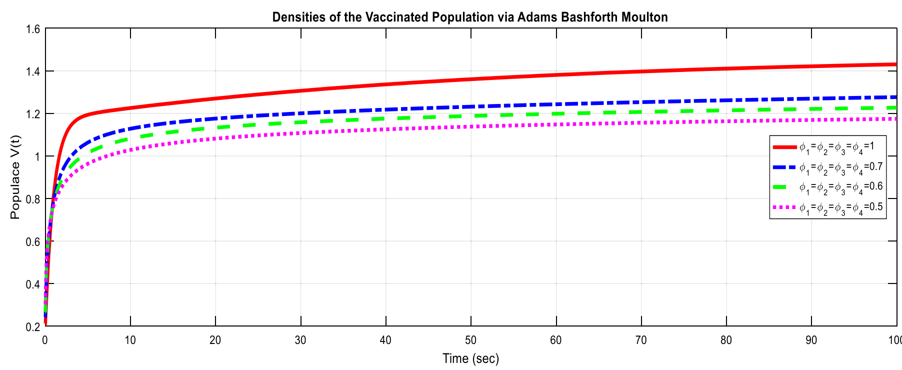


**Figure 28** Dynamic of populace *V*(*t*) by varying the value of $\phi$

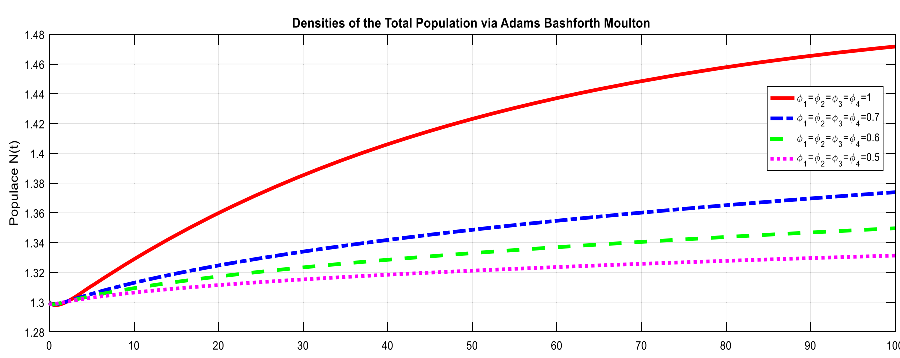


**Figure 29** Dynamic of populace *N*(*t*) by varying the value of $\phi$

We can discretize (17) with the PWCA method as follows:

$$\begin{cases} D^{\phi_1} S(t) = b - \beta(1-\mu_1)S([\tfrac{t}{s}]s)I([\tfrac{t}{s}]s) - (d+\mu_1)S([\tfrac{t}{s}]s), \\ D^{\phi_1} I(t) = \beta(1-\mu_1)S([\tfrac{t}{s}]s)I([\tfrac{t}{s}]s) - (d+\mu_2+\alpha)I([\tfrac{t}{s}]s), \\ D^{\phi_1} V(t) = \mu_1 S([\tfrac{t}{s}]s) - dV([\tfrac{t}{s}]s), \\ D^{\phi_1} N(t) = b - N([\tfrac{t}{s}]s)d - \alpha I([\tfrac{t}{s}]s). \end{cases} \tag{26}$$

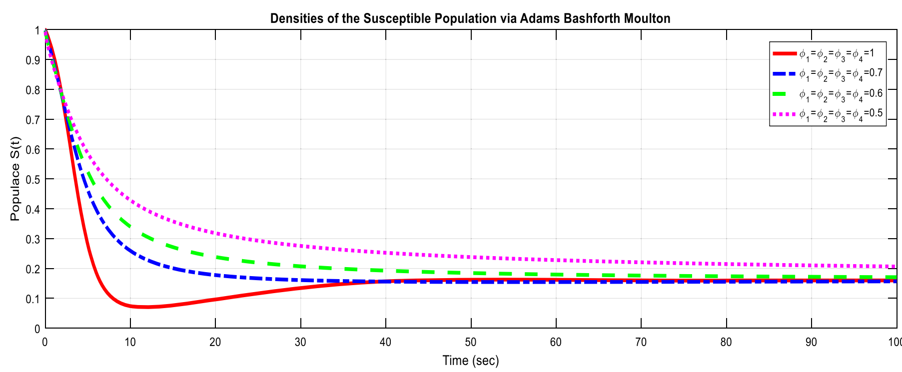


**Figure 30** Dynamic of populace $S(t)$ by varying the value of $\phi$

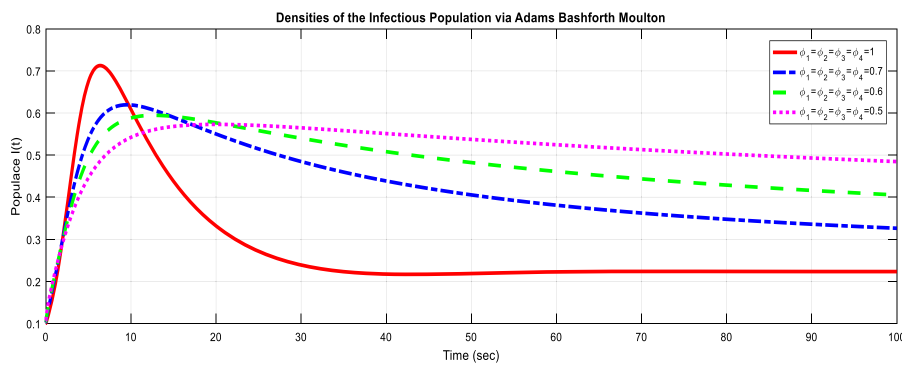


**Figure 31** Dynamic of populace $I(t)$ by varying the value of $\phi$

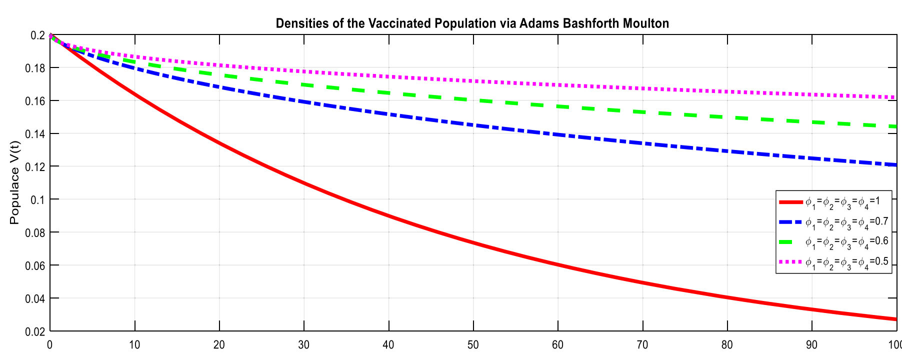


**Figure 32** Dynamic of populace $V(t)$ by varying the value of $\phi$

First, let $t \in [0, s)$, i.e., $\frac{t}{s} \in [0, 1)$. Thus, we obtain

$$\begin{cases} D^{\phi_1} S(t) = b - \beta(1-\mu_1)S(0)I(0) - (d+\mu_1)S(0), \\ D^{\phi_2} I(t) = \beta(1-\mu_1)S(0)I(0) - (d+\mu_2+\alpha)I(0), \\ D^{\phi_3} V(t) = \mu_1 S(0) - dV(0), \\ D^{\phi_4} N(t) = b - N(0)d - \alpha I(0), \end{cases} \tag{27}$$

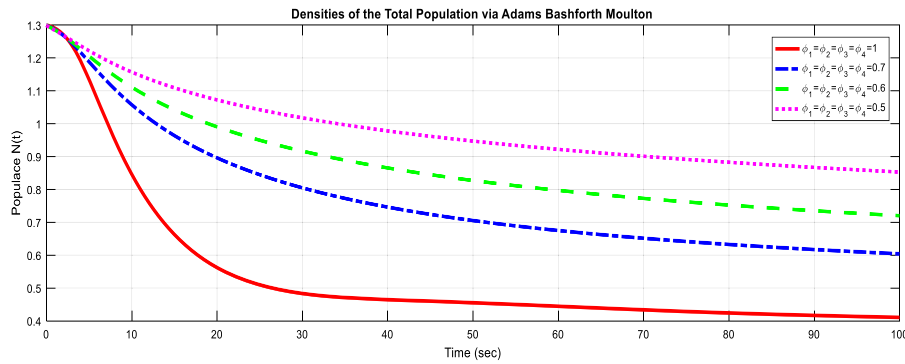


**Figure 33** Dynamic of populace $N(t)$ by varying the value of $\phi$

**Table 1** Parameters used for Numerical study

| Parameters | Values | |
|---|---|---|
| | DFE | EE |
| $\beta$ | 0.75 | 0.75 |
| $b$ | 0.03 | 0.03 |
| $d$ | 0.02 | 0.02 |
| $\mu_1$ | 1 | 0 |
| $\mu_2$ | 1 | 0 |
| $\alpha$ | 0.1 | 0.1 |

and the solution of (27) is reduced to

$$\begin{cases} S_1(t) = S(0) + J^{\phi_1}(b - \beta(1-\mu_1)S(0)I(0) - (d+\mu_1)S(0)), \\ I_1(t) = I(0) + J^{\phi_2}(\beta(1-\mu_1)S(0)I(0) - (d+\mu_2+\alpha)I(0)), \\ V_1(t) = V(0) + J^{\phi_3}(\mu_1 S(0) - dV(0)), \\ N_1(t) = N(0) + J^{\phi_4}(b - N(0)d - \alpha I(0)), \end{cases}$$
$$\begin{cases} S_1(t) = S(0) + \frac{t^{\phi_1}}{\phi_1\Gamma(\phi_1)}(b - \beta(1-\mu_1)S(0)I(0) - (d+\mu_1)S(0)), \\ I_1(t) = I(0) + \frac{t^{\phi_2}}{\phi_2\Gamma(\phi_2)}(\beta(1-\mu_1)S(0)I(0) - (d+\mu_2+\alpha)I(0)), \\ V_1(t) = V(0) + \frac{t^{\phi_3}}{\phi_3\Gamma(\phi_3)}(\mu_1 S(0) - dV(0)), \\ N_1(t) = N(0) + \frac{t^{\phi_4}}{\phi_4\Gamma(\phi_4)}(b - N(0)d - \alpha I(0)), \end{cases} \tag{28}$$

second, let $t \in [s, 2s)$, i.e., $\frac{t}{s} \in [1, 2)$. Thus, we obtain

$$\begin{cases} D^{\phi_1}S(t) = b - \beta(1-\mu_1)S_1(t)I_1(t) - (d+\mu_1)S_1(t), \\ D^{\phi_2}I(t) = \beta(1-\mu_1)S_1(t)I_1(t) - (d+\mu_2+\alpha)I_1(t), \\ D^{\phi_3}V(t) = \mu_1 S_1(t) - dV_1(t), \\ D^{\phi_4}N(t) = b - N_1(t)d - \alpha I_1(t), \end{cases} \tag{29}$$

which has the following solution:

$$\begin{cases} S_2(t) = S_1(s) + J^{\phi_1}(b - \beta(1-\mu_1)S_1(s)I_1(s) - (d+\mu_1)S_1(s)), \\ I_2(t) = I_1(s) + J^{\phi_2}(\beta(1-\mu_1)S_1(s)I_1(s) - (d+\mu_2+\alpha)I_1(s)), \\ V_2(t) = V_1(s) + J^{\phi_3}(\mu_1 S_1(s) - dV_1(s)), \\ N_2(t) = N_1(s) + J^{\phi_4}(b - N_1(s)d - \alpha I_1(s)), \end{cases}$$
$$\begin{cases} S_2(t) = S_1(s) + \frac{t^{\phi_1}}{\phi_1\Gamma(\phi_1)}(b - \beta(1-\mu_1)S_1(s)I_1(s) - (d+\mu_1)S_1(s)), \\ I_2(t) = I_1(s) + \frac{t^{\phi_2}}{\phi_2\Gamma(\phi_2)}(\beta(1-\mu_1)S_1(s)I_1(s) - (d+\mu_2+\alpha)I_1(s)), \\ V_2(t) = V_1(s) + \frac{t^{\phi_3}}{\phi_3\Gamma(\phi_3)}(\mu_1 S_1(s) - dV_1(s)), \\ N_2(t) = N_1(s) + \frac{t^{\phi_4}}{\phi_4\Gamma(\phi_4)}(b - N_1(s)d - \alpha I_1(s)), \end{cases} \tag{30}$$

where $J_s^{\alpha_i} = \frac{1}{\Gamma(\alpha_i)}\int_s^\tau (t-p)^{\alpha_i-1}\,dp$, $0 < \alpha_i \leq 1$ and $i = 1,2,3,4$. Thus after repeating the discretization process $n$ times, we obtain the discretized form of system (17) as follows:

$$\begin{cases} S_{n+1}(t) = S_n(ns) + \frac{t^{\phi_1}}{\phi_1\Gamma(\phi_1)}(b - \beta(1-\mu_1)S_n(ns)I_n(ns) - (d+\mu_1)S_n(ns)), \\ I_{n+1}(t) = I_n(ns) + \frac{t^{\phi_2}}{\phi_2\Gamma(\phi_2)}(\beta(1-\mu_1)S_n(ns)I_n(ns) - (d+\mu_2+\alpha)I_n(ns)), \\ V_{n+1}(t) = V_n(ns) + \frac{t^{\phi_3}}{\phi_3\Gamma(\phi_3)}(\mu_1 S_n(ns) - dV_n(ns)), \\ N_{n+1}(t) = N_n(ns) + \frac{t^{\phi_4}}{\phi_4\Gamma(\phi_4)}(b - N_n(ns)d - \alpha I_n(ns)), \end{cases} \tag{31}$$

where $t \in [ns, (n+1)s)$. For $t \to (n+1)s$, the system (31) is reduced to

$$\begin{cases} S_{n+1}(t) = S_n + \frac{t^{\phi_1}}{\phi_1\Gamma(\phi_1)}(b - \beta(1-\mu_1)S_nI_n - (d+\mu_1)S_n), \\ I_{n+1}(t) = I_n + \frac{t^{\phi_2}}{\phi_2\Gamma(\phi_2)}(\beta(1-\mu_1)S_nI_n - (d+\mu_2+\alpha)I_n), \\ V_{n+1}(t) = V_n + \frac{t^{\phi_3}}{\phi_3\Gamma(\phi_3)}(\mu_1 S_n - dV_n), \\ N_{n+1}(t) = N_n + \frac{t^{\phi_4}}{\phi_4\Gamma(\phi_4)}(b - N_nd - \alpha I_n). \end{cases} \tag{32}$$

It should be noticed that if $\phi_i \to 1$ ($i = 1,2,3,4$) in (32), we obtain the corresponding Euler discretization of the discretized measles model with commensurate order. It is different from the predictor corrector method. The obtained result is a four dimensional discrete system.

According to Angstmann *et al.* [35], the generalized Euler method (GEM) and piece wise continuous argument (PCWA) methods do not give the proper results, which is why we also used two other techniques (the Adams–Bashforth–Moulton method and the Grunwald–Letnikov method) to show the efficiency of the measles model in Sects. 4.3 and 4.4.

### 4.3 Grunwald–Letnikov method (Binomial Coefficients)

For numerical use of the non-integer order derivative we can use Eq. (33) resulting from the Grunwald–Letnikov approach. This tactic is centered on the point that, for a wide-ranging class of functions, two approaches, the Grunwald Letnikov definition and the Caputo definition, are comparable. The relation for the explicit numerical approximation of

$\varphi$th derivative at the points $kh$ ($k = 1, 2, \dots$) has the following form [6]:

$$_{(k-L/h)}D^{\varphi}_{t_k} f(t) \approx \frac{1}{h^{\varphi}} \sum_{j=0}^{k} (-1)^j \binom{\varphi}{j} f(t_{k-j}), \tag{33}$$

where $L$ is the "memory length", $t_k = kh$, $h$ is the time step and the $(-1)^j\binom{\varphi}{j}$ are the binomial coefficients $C^{(\varphi)}_j$ ($j = 0, 1, 2, \dots$). For them we can use the expression [6]

$$C^{(\varphi)}_0 = 1, \qquad C^{(\varphi)}_j = \left(1 - \frac{1+\varphi}{j}\right) C^{(\varphi)}_{j-1}.$$

Then the common numerical elucidation of the non-integer differential equation

$$_aD^{\varphi}_t y(t) = f\big(t, y(t)\big)$$

can be written as

$$y(t_k) = f\big(t_k, y(t_k)\big) h^{\varphi} - \sum_{j=0}^{k} C^{(\varphi)}_j y(t_{k-j}).$$

Now we express system (17) in the above format,

$$S(t_k) = \big\{b - \beta(1-\mu_1)S(t_{k-1})I(t_{k-1}) - (d+\mu_1)S(t_{k-1})\big\} h^{\phi_1} - \sum_{j=1}^{k} C^{(\phi_1)}_j S(t_{k-j}),$$

$$I(t_k) = \big\{\beta(1-\mu_1)S(t_k)I(t_{k-1}) - (d+\mu_2+\alpha)I(t_{k-1})\big\} h^{\phi_2} - \sum_{j=1}^{k} C^{(\phi_2)}_j I(t_{k-j}),$$

$$V(t_k) = \big\{\mu_1 S(t_k) - dV(t_{k-1})\big\} h^{\phi_3} - \sum_{j=1}^{k} C^{(\phi_3)}_j V(t_{k-j}),$$

$$N(t_k) = \big\{b - dN(t_{k-1}) - \alpha I(t_k)\big\} h^{\phi_3} - \sum_{j=1}^{k} C^{(\phi_3)}_j N(t_{k-j}),$$

where $C^{(\phi_i)}_0 = 1$, $C^{(\phi_i)}_j = (1 - \frac{1+\phi_i}{j}) C^{(\phi_i)}_{j-1}$, $i = 1, 2, 3, 4$.

### 4.4 Adams–Bashforth–Moulton method

One can use the generalized Adams–Bashforth–Moulton method for numerical solutions of the system (17) (see [6]).

So

$$\begin{aligned} S^{n+1} &= S(0) + \frac{h^{\phi_1}}{\Gamma(\phi_1+2)}\big(b - \beta(1-\mu_1)S^p_{n+1}I^p_{n+1} - (d+\mu_1)S^p_{n+1}\big) \\ &\quad + \frac{h^{\phi_1}}{\Gamma(\phi_1+2)} \sum_{l=0}^{n} a_{l,n+1}\big(b - \beta(1-\mu_1)S_l I_l - (d+\mu_1)S_l\big), \end{aligned}$$

$$
\begin{aligned}
I^{n+1} &= I(0) + \frac{h^{\phi_2}}{\Gamma(\phi_2+2)}\big(\beta(1-\mu_1)S^p_{n+1}I^p_{n+1} - (d+\mu_2+\alpha)I^p_{n+1}\big) \\
&\quad + \frac{h^{\phi_2}}{\Gamma(\phi_2+2)}\sum_{l=0}^{n} a_{l,n+1}\big(\beta(1-\mu_1)S_lI_l - (d+\mu_2+\alpha)I_l\big), \\
V^{n+1} &= V(0) + \frac{h^{\phi_3}}{\Gamma(\phi_3+2)}\big(\mu_1 S^p_{n+1} - dV^p_{n+1}\big) \\
&\quad + \frac{h^{\phi_3}}{\Gamma(\phi_3+2)}\sum_{l=0}^{n} a_{l,n+1}(\mu_1 S_l - dV_l), \\
N^{n+1} &= N(0) + \frac{h^{\phi_3}}{\Gamma(\phi_3+2)}\big(b - dN^p_{n+1} - \alpha I^p_{n+1}\big) \\
&\quad + \frac{h^{\phi_3}}{\Gamma(\phi_3+2)}\sum_{l=0}^{n} a_{l,n+1}(b - dN_l - \alpha I_l),
\end{aligned}
$$

where

$$
\begin{aligned}
S^p_{n+1} &= S(0) + \frac{1}{\Gamma(\phi_1)}\sum_{l=0}^{n} b_{l,n+1}\big(b - \beta(1-\mu_1)S_lI_l - (d+\mu_1)S_l\big), \\
I^p_{n+1} &= I(0) + \frac{1}{\Gamma(\phi_2)}\sum_{l=0}^{n} b_{l,n+1}\big(\beta(1-\mu_1)S_lI_l - (d+\mu_2+\alpha)I_l\big), \\
V^p_{n+1} &= V(0) + \frac{1}{\Gamma(\phi_3)}\sum_{l=0}^{n} b_{l,n+1}(\mu_1 S_l - dV_l), \\
N^p_{n+1} &= N(0) + \frac{1}{\Gamma(\phi_3)}\sum_{l=0}^{n} b_{l,n+1}(b - dN_l - \alpha I_l),
\end{aligned}
$$

with

$$
a_{l,n+1} = \begin{cases} n^{\phi_i+1} - (n-\phi_i)(n+1)^{\phi_i}, & l = 0, \\ (n-l+2)^{\phi_i+1} + (n-l)^{\phi_i+1} - 2(n-l+1)^{\phi_i+1}, & 1 \le l \le n, \\ 1, & l = n+1, \end{cases}
$$

and

$$
b_{l,n+1} = \frac{h^{\phi_i}}{\phi_i}\big((n-l+1)^{\phi_i} - (n-l)^{\phi_i}\big), \quad 0 \le l \le n
$$

with $i = 1, 2, 3, 4$.

## 5 Conclusion

In this paper, a non-linear mathematical Measles model with fractional order $\phi_i$, $i = 1, 2, \dots, 4$ is formulated. The stability of both the DFE and the EE points is discussed. Sufficient conditions for local stability of the DFE point $\mathcal{F}_0$ are given in terms of the basic reproduction number $\mathcal{R}_0$ of the model, where it is asymptotically stable if $\mathcal{R}_0 < 1$. The positive infected equilibrium $\mathcal{F}^*$ exists when $\mathcal{R}_0 > 1$ and sufficient conditions that guarantee the asymptotic stability of this point are given. Beside this sensitivity analysis of the parameters involved the threshold parameter ($\mathcal{R}_0$) is discussed. Considering three fractional order techniques, we actually checked the best performance wise efficiency of the model. When simulating the model with all four algorithms, we have observed that all methods are converging to disease free and endemic equilibrium points but through different paths for diverse values of $\phi$. The values are very close to each other in all three techniques. However, the time consumed (Core i7 Desktop) by GEM is 10 sec, PWCA is 43 sec, Grunwald–Letnikov (binomial coefficient) is 7716.97 sec, and the Adams–Bashforth–Moulton algorithm is 87,326.743 sec, which indicates that the computational cost for GEM is lower than the rests. Measles is an infectious disease highly contagious from person to person occurring during childhood. So, the main goal of analyzing such techniques for a measles model is to benefit the researchers and policy makers in targeting, in preclusion and in treatment resources for supreme effectiveness. Also the length of time of approaching equilibrium within a given tolerance is interesting. The early transient behaviors vary greatly among the methods. Each method converges to the same disease free and endemic equilibrium points. For different values of $\phi_i$, $i = 1, \ldots, 4$, the system approaches the same equilibrium point but through different paths. Numerical studies with diverse order show that the system decays to equilibrium with a power, $t^{-\phi}$. The outcome shows an important picture of the use of non-integer order to model the SIRV. The fractional order may offer extra 'freedom' to fine-tune the model to real data from particular patients. Specifically, the fractional order index contributes positively to better fits of the patients' data.

**Acknowledgements**
We would like to thank the referees for their valuable comments.

**Funding**
No funding is available for this research project.

**Availability of data and materials**
Not applicable.

**Ethics approval and consent to participate**
Not applicable.

**Competing interests**
The authors declare that they have no competing interests.

**Consent for publication**
Not applicable.

**Authors' contributions**
The authors equally have made contributions. All authors read and approved the manuscript.

**Author details**
[1]Department of Mathematics, University of Engineering and Technology, Lahore, Pakistan. [2]Faculty of Information Technology, University of Central Punjab, Lahore, Pakistan. [3]Department of Mathematics, University of Engineering and Technology, KSK Campus, Lahore, Pakistan.

## Publisher's Note
Springer Nature remains neutral with regard to jurisdictional claims in published maps and institutional affiliations.

Received: 27 February 2019 Accepted: 30 July 2019 Published online: 09 August 2019

**References**
1. Schaffer, W.M., Kot, M.: Nearly one dimensional dynamics in an epidemic. J. Theor. Biol. **112**, 403–427 (1985)
2. WHO, Department of Vaccines and Biologicals, Measles Technical Working Group: Strategies for Measles control and Elimination, Report of a meeting Geneva, Switzerland (2012)

3. Zafar, Z., Rehan, K., Mushtaq, M., Rafiq, M.: Numerical treatment for nonlinear brusselator chemical model. J. Differ. Equ. Appl. **23**(3), 521–538 (2017)
4. Zafar, Z., Rehan, K., Mushtaq, M., Rafiq, M.: Numerical modeling for nonlinear biochemical reaction networks. Iran. J. Math. Chem. **8**(4), 413–423 (2017)
5. Zafar, Z., Ahmad, M.O., Pervaiz, A., Rafiq, M.: Fourth order compact method for one dimensional inhomogeneous telegraph equations with $O(h4, k3)$. Pak. J. Eng. Appl. Sci. **14**, 96–101 (2014)
6. Zafar, Z., Rehan, K., Mushtaq, M.: HIV/AIDS epidemic fractional-order model. J. Differ. Equ. Appl. **23**(7), 1298–1315 (2017)
7. Zafar, Z., Mushtaq, M., Rehan, K.: A non-integer order dengue internal transmission model. Adv. Differ. Equ. **2018**, Article ID 23 (2018)
8. Arafa, A.A.M., Rida, S.Z., Khalil, M.: A fractional-order of HIV infection with drug therapy effect. J. Egypt. Math. Soc. **22**(3), 538–543 (2014)
9. Li, H.L., Zhang, L., Hu, C., Jiang, Y.L., Teng, Z.: Dynamical analysis of a fractional- order predator-prey model incorporating a prey refuge. J. Appl. Math. Comput. **54**, 435–449 (2017)
10. Goufo, E.F.D., Martiz, R., Munganga, J.: Some properties of the Kermack McKendrick epidemic model with fractional derivative and nonlinear incidence. Adv. Differ. Equ. **2014**, Article ID 278 (2014)
11. Dokoumetzidis, A., Magin, R., Macheras, P.: A commentary on fractionalization of multi-compartmental models. J. Pharmacokinet. Pharmacodyn. **37**, 203–207 (2010)
12. Angstmann, C.N., Magin, R., Macheras, P.: A fractional order recovery SIR model from a stochastic process. Bull. Math. Biol. **78**, 468–499 (2016)
13. Angstmann, C.N., Henry, B.I., McGann, A.V.: A fractional order infectivity SIR model. Phys. A, Stat. Mech. Appl. **452**, 86–93 (2016)
14. Angstmann, C.N., Erickson, A.M., Henry, B.I., McGann, A.V., Murray, J.M., Nicholas, J.A.: Fractional order compartment models. SIAM J. Appl. Math. **77**(2), 430–446 (2017)
15. Sardar, T., Saha, B.: Mathematical analysis of a power–law form time dependent vector- born disease transmission model. Math. Biosci. **288**, 109–123 (2017)
16. Matignon, D.: Stability results for fractional differential equations with applications to control processing. Comput. Eng. Sys. Appl. **2**, 963 (1996)
17. https://www.who.int/immunization/newsroom/measles-data-2019/en/. Accessed 17 June 2019
18. https://www.who.int/en/news-room/fact-sheets/detail/measles. Accessed 17 June 2019
19. World health organization: The World Health Report 2001 – Mental Health New Understanding, New Hope. WHO, Geneva (2001)
20. Zafar, Z., Rehan, K., Mushtaq, M.: Fractional-order scheme for bovine babesiosis disease and tick populations. Adv. Differ. Equ. **2017**, Article ID 86 (2017)
21. Zafar, Z.: Fractional order Lengyel–Epstein chemical reaction model. Comput. Appl. Math. **38**, 131 (2019)
22. Machado, T.R., Kiryakova, V., Mainardi, F.: Recent history of fractional calculus. Commun. Nonlinear Sci. Numer. Simul. **16**, 1140–1153 (2011)
23. Momoh, A.A., Ibrahim, M.O., Uwanta, I.J., Manga, S.B.: Mathematical model for control of measles epidemiology. Int. J. Pure Appl. Math. **87**(5), 707–718 (2013)
24. David, Y.: The analysis of vaccination and treatment of Measles diseases described by a fractional order SIR epidemiology model. 2014 M. Phil Thesis
25. Isea, R., Lonngren, K.E.: Epidemaic modeling using data from the 2001–2002 measles outbreak in venezuella. Res. Rev. Biosci. **7**(1), 15–18 (2013)
26. Peter, O.J., Afolabi, O.A., Victor, A.A., Akpan, C.E., Oguntolu, F.A.: Mathematical model for the control of measles. J. Appl. Sci. Environ. Manag. **22**(4), 571–576 (2018)
27. Yaro, D., Omari-Sasu, S.K., Harvin, P., Saviour, A.W., Obeng, B.A.: Generalized Euler method for modeling measles with fractional differential equations. Int. J. Innov. Res. Dev. **4**(4), 358–366 (2015)
28. Odibat, Z., Moamni, S.: An algorithm for the numerical solution of differential equations of fractional order. J. Appl. Math. Inform. **26**, 15–27 (2008)
29. Odibat, Z., Shawagfeh, N.: Generalized Taylor's formula. Appl. Math. Comput. **186**, 286–293 (2007)
30. Arafa, A.A.M., Rida, S.Z., Khalil, M.: A fractional-order model of HIV infection: numerical solution and comparisons with data of patients. Int. J. Biomath. **7**(4), 1450036 (2014)
31. Arafa, A.A.M., Rida, S.Z., Khalil, M.: The effect of anti-viral drug treatment of human immunodeficiency virus type 1 (HIV-1) described by a fractional order model. Appl. Math. Model. **37**(4), 2189–2196 (2013)
32. Arafa, A.A.M., Rida, S.Z., Khalil, M.: Fractional modeling dynamics of HIV and CD4+ T-cells during primary infection. EPJ Nonlinear Biomed. Phys. **6**(1), 1–7 (2012)
33. El-Sayed, A.M.A., El-Rehman, Z.F., Salman, S.M.: Discretization of forced Duffing oscillator with fractional-order damping. Adv. Differ. Equ. **2014**), 66 (2014)
34. Agarwal, R.P., El-Sayed, A.M.A., Salman, S.M.: Fractional order Chua's system: discretization, bifurcation and chaos. Adv. Differ. Equ. **2013**, 320 (2013)
35. Angstmann, C.N., Henry, B.I., Jacobs, B.A., McGann, A.V.: Discretization of Fractional Differential Equations by a Piecewise Continuous Approximation. J. Comput. Phys. (2016) arXiv:1605.01815v1 [math.NA]
36. Kaninda, A.V., Legros, D., Jataou, I.M., Malfait, P., Maisonneuve, M., Paquet, C., Moren, A.: Measles vaccine effectiveness in standard and early immunization strategies, Niger. Pediatr. Infect. Dis. J. **17**, 1034–1039 (1998)
37. Allen, L.J.S.: An Introduction to Mathematical Biology. Pearson Education, Upper Saddle River (2007)